UDC 551.509.313

A THEORETICAL INTERPRETATION OF ANISOTROPICALLY WEIGHTED SMOOTHING ON THE BASIS OF NUMERICAL VARIATIONAL ANALYSIS

YOSHIKAZU SASAKI

The University of Oklahoma, Norman, Okla.

ABSTRACT

The weighting factors used in conventional objective analysis methods are reviewed on the basis of numerical variational analysis. Special emphasis is placed on anisotropy (ellipticity) of the factors. The weighting factors of the objective analysis methods were empirically determined and are two dimensional in a horizontal plane (x, y). Most of these weighting factors are isotropic. However, anisotropic weighting factors have recently been used to give greater weight to the upstream and downstream observations as compared to those of the crosswind direction.

A simple advection equation is used as a dynamical constraint in the numerical variational analysis in order to take into account quantitatively the effect of wind direction and speed on the anisotropy. A simple low-pass filter is also included in the variational formalism. A Green's function, derived for the Eular equation, is used to discuss the theoretical basis of the isotropic and anisotropic weighting factors.

The results obtained from the numerical variational analysis scheme suggest that the weights for the upstream and downstream observations should be of the same magnitude and as much as three times larger than the respective weights for the crosswind direction. These results were obtained by taking time t as a constant and considering a reasonable range of wind speeds. These suggestions seem to support the empirical anisotropic weighting factors proposed by Endlich and Mancuso. Additional discussion concerns weighting along the time coordinate simultaneously with the two space coordinates.

1. INTRODUCTION

Endlich and Mancuso (1968) suggested a modification of the Cressman objective analysis scheme (Cressman 1959) in which greater weight would be applied to both upwind and downwind observations as compared to those of crosswind direction. Inman (1970) recently developed this scheme into a form for operational use. The modification seems to improve the accuracy and details of analyzed patterns near such features as the low-level jet axes. These features are obviously important for local weather analysis and forecasting, but are especially vital for severe-storm forecasting.

The theoretical foundation for anisotropic weighting is of interest. Determination of these weights on a dynamical basis should have not only theoretical interest but should also have value for further development of objective analysis techniques. A variational analysis method (Sasaki 1970*a*, 1970*b*) is used in this study as a basis for developing a theoretical foundation of anisotropically weighted smoothing. Furthermore, this study extends the analysis of spatial weighting to include a proper weight for the time coordinate relative to those of the space coordinates. The discussion is illustrated by taking an advection equation as a dynamical constraint of the numerical variational analysis.

2. NUMERICAL VARIATIONAL ANALYSIS WITH A SIMPLE ADVECTION EQUATION

The variational equation in a continuous system, using advection as a "weak constraint" (Sasaki 1970*a*, 1970*b*) is

$$\delta J=\delta\iiint\left\{\tilde{\alpha}'(\varphi'-\tilde{\varphi}')^2+\alpha'\left(\frac{\partial}{\partial t'}\varphi'+c_x'\frac{\partial}{\partial x'}\varphi'+c_y'\frac{\partial}{\partial y'}\varphi'\right)^2+\alpha_t'\left(\frac{\partial}{\partial t'}\varphi'\right)^2+\alpha_s'\left(\frac{\partial}{\partial x'}\varphi'\right)^2+\alpha_s'\left(\frac{\partial}{\partial y'}\varphi'\right)^2\right\}dt'dx'dy'=0 \quad (1)$$

where J is the functional, $\tilde{\alpha}'$, α', α_t', and α_s' are the prespecified weights (may be functions of t', x', and y' but assumed as constants in this study); φ' is a function of t', x', and y'; $\frac{\partial}{\partial t'}$, $\frac{\partial}{\partial x'}$, and $\frac{\partial}{\partial y'}$ are the first derivatives with respect to t', x', and y', respectively. The x' and y' components of wind velocity, c_x' and c_y' respectively, are assumed to be prespecified constants (can also be functions of t', x', and y'). Discussion centers on the continous system in this study, but an extension to a discrete system can be made (Sasaki 1970*b*).

The first term of the right-hand side of eq (1) is the "observational constraint" (minimizing the variance between the observation and analyzed field), the second term is the "weak dynamical constraint", namely,

$$\frac{\partial}{\partial t'}\varphi'+c_x'\frac{\partial}{\partial x'}\varphi'+c_y'\frac{\partial}{\partial y'}\varphi'\doteq 0. \quad (2)$$

The word *weak* is used because the advection equation is assumed to be approximately rather than rigorously satisfied. If rigorous satisfaction of the advection equation is required, then other variational formalisms should be used (Sasaki 1970*a*). The approximation form is more compatible with the *empirical* determination of aniso-

tropic weights in the objective analyses. The third term of eq (1) is a low-pass filter of frequency. The fourth and fifth terms are low-pass filters of wave numbers. The second term of eq (1) also behaves as a filter for suppressing the magnitude of disturbances that move with translation velocities different from those specified by c_x', and c_y'. The greater the difference is, the more the magnitude is suppressed (Sasaki 1970*b*). The purpose of including the third, fourth, and fifth terms of eq (1) is not only to remove undesirable high-frequency and high-wave number components but also to eliminate any possible discontinuity of the analyzed field. If only the first and second terms of eq (1) are used, discontinuity of solution may appear in the direction normal to a streamline defined by the velocity components c_x' and c_y' (Sasaki 1970*a*). An aim of conventional objective analyses is to obtain smooth analyzed patterns and such a discontinuity is not desirable. Therefore, the low-pass filters expressed by the third, fourth, and fifth terms of eq (1) are included.

Equation (1) is nondimensionalized by defining the charateristic scales Φ for φ', τ for t', L for x' and y', L/τ for c_x' and c_y', $1/\Phi^2$ for $\tilde{\alpha}'$, τ^2/Φ^2 for α', and L^2/Φ^2 for α_s' as follows:

$$\begin{aligned}
\varphi' &= \Phi\varphi, \\
t' &= \tau t, \\
x' &= Lx, \\
y' &= Ly, \\
c_x' &= \frac{L}{\tau} c_x, \\
c_y' &= \frac{L}{\tau} c_y, \\
\tilde{\alpha}' &= \frac{1}{\Phi^2}\tilde{\alpha}, \\
\alpha' &= \frac{\tau^2}{\Phi^2}\alpha, \\
\text{and} \qquad & \\
\alpha_s' &= \frac{L^2}{\Phi^2}\alpha_s
\end{aligned} \tag{3}$$

where φ, t, x, y, c_x, c_y, $\tilde{\alpha}$, α, and α_s are nondimensional variables. If one uses eq (3), eq (1) can be written in a nondimensional form as

$$\delta J = \delta \iiint \left\{ \tilde{\alpha}(\varphi-\tilde{\varphi})^2 + \alpha\left(\frac{\partial}{\partial t}\varphi + c_x\frac{\partial}{\partial x}\varphi + c_y\frac{\partial}{\partial y}\varphi\right)^2 + \alpha_t\left(\frac{\partial}{\partial t}\varphi\right)^2 + \alpha_s\left[\left(\frac{\partial}{\partial x}\varphi\right)^2 + \left(\frac{\partial}{\partial y}\varphi\right)^2\right]\right\} dtdxdy = 0. \tag{4}$$

The Euler-Lagrange equation (also called the Euler equation) is derived from eq (4). This equation is

$$\tilde{\alpha}(\varphi-\tilde{\varphi}) - \alpha\left(\frac{\partial}{\partial t}+c_x\frac{\partial}{\partial x}+c_y\frac{\partial}{\partial y}\right)\left(\frac{\partial}{\partial t}+c_x\frac{\partial}{\partial x}+c_y\frac{\partial}{\partial y}\right)\varphi - \alpha_t\frac{\partial^2}{\partial t^2}\varphi - \alpha_s\left(\frac{\partial^2}{\partial x^2}+\frac{\partial^2}{\partial y^2}\right)\varphi = 0. \tag{5}$$

This is a second-order partial differential equation of the elliptic type if α_t and α_s are not zero (Sasaki 1970*b*).

For simplicity, we assume that $c_x=0$ and $c_y\neq 0$. This assumption does not detract from the generality of the discussion as it can be achieved by a proper coordinate transformation. Under this assumption eq (5) is written as

$$\tilde{\alpha}(\varphi-\tilde{\varphi}) - \alpha\left(\frac{\partial}{\partial t}+c_y\frac{\partial}{\partial y}\right)\left(\frac{\partial}{\partial t}+c_y\frac{\partial}{\partial y}\right)\varphi - \alpha_t\frac{\partial^2}{\partial t^2}\varphi - \alpha_s\left(\frac{\partial^2}{\partial x^2}+\frac{\partial^2}{\partial y^2}\right)\varphi = 0. \tag{6}$$

3. STANDARD FORM OF EQUATION (6)

A set of new orthogonal coordinates is chosen in order to transform eq (6) into a standard form of elliptic type of differential equation. Since the only derivatives in eq (6) with respect to x are $\partial^2/\partial x^2$, the coordinate transformation, $(x, y, t)\rightarrow(X, Y, T_1)$, is performed on the y-t plane; and, therefore, the x-coordinate is unchanged as shown in figure 1;

$$\begin{aligned}
X &= x, \\
Y &= y\cos\theta - t\sin\theta, \\
\text{and} \qquad & \\
T_1 &= y\sin\theta + t\cos\theta.
\end{aligned} \tag{7}$$

Using this transformation, eq (6) becomes

$$\begin{aligned}
&\alpha\left[(-\sin\theta+c_y\cos\theta)^2\frac{\partial^2}{\partial Y^2} + (\cos\theta+c_y\sin\theta)^2\frac{\partial^2}{\partial T_1^2} + 2(-\sin\theta+c_y\cos\theta)(\cos\theta+c_y\sin\theta)\frac{\partial^2}{\partial Y\partial T_1}\right]\varphi \\
&+\alpha_t\left[\sin^2\theta\frac{\partial^2}{\partial Y^2} + \cos^2\theta\frac{\partial^2}{\partial T_1^2} - \sin\theta\cos\theta\frac{\partial^2}{\partial Y\partial T_1}\right]\varphi \\
&+\alpha_s\frac{\partial^2\varphi}{\partial X^2} + \alpha_s\left[\cos^2\theta\frac{\partial^2}{\partial Y^2} + \sin^2\theta\frac{\partial^2}{\partial T_1^2} - \cos\theta\sin\theta\frac{\partial^2}{\partial Y\partial T_1}\right]\varphi = \tilde{\alpha}(\varphi-\tilde{\varphi})
\end{aligned} \tag{8}$$

or

$$\begin{aligned}
&\alpha_s\frac{\partial^2\varphi}{\partial X^2} + [\alpha(-\sin\theta+c_y\cos\theta)^2 + \alpha_t\sin^2\theta + \alpha_s\cos^2\theta]\frac{\partial^2\varphi}{\partial Y^2} \\
&+[\alpha(\cos\theta+c_y\sin\theta)^2 + \alpha_t\cos^2\theta + \alpha_s\sin^2\theta]\frac{\partial^2\varphi}{\partial T_1^2} \\
&+[2\alpha(-\sin\theta+c_y\cos\theta)(\cos\theta+c_y\sin\theta) - (\alpha_t-\alpha_s) \\
&\times\sin\theta\cos\theta]\frac{\partial^2\varphi}{\partial Y\partial T_1} = \tilde{\alpha}(\varphi-\tilde{\varphi})
\end{aligned} \tag{8'}$$

where θ is the angle between the y and Y coordinates or t and T_1 coordinates.

For simplicity, we assume

$$\alpha_t = \alpha_s (\equiv \alpha_f) \tag{9}$$

and

$$\theta = \tan^{-1} c_y; \tag{10}$$

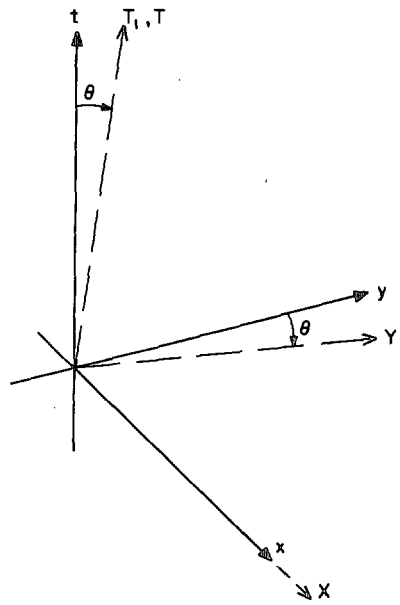

FIGURE 1.—Transformation of coordinates (x,y,t) to (X,Y,T_1) on the y-t plane, eq (6).

θ is positive for clockwise rotation around the x-axis and represents the angle between the time coordinate and the characteristic line defined from $\partial\varphi/\partial t+c_y\,\partial\varphi/\partial y=0$.

By these assumptions, eq (8) or (8′) is simplified to the form

$$\alpha_f\frac{\partial^2\varphi}{\partial X^2}+\alpha_f\frac{\partial^2\varphi}{\partial Y^2}+(a+\alpha_f)\frac{\partial^2\varphi}{\partial T_1^2}-\tilde{\alpha}\varphi=-\tilde{\alpha}\tilde{\varphi} \tag{11}$$

where

$$a=\alpha(\cos\theta+c_y\sin\theta). \tag{12}$$

Equation (11) is standardized when we adopt an expanded coordinate T that is defined as

$$T=\left(\frac{\alpha_f}{a+\alpha_f}\right)^{1/2}T_1. \tag{13}$$

The final standard form becomes

$$\left(\frac{\partial^2}{\partial X^2}+\frac{\partial^2}{\partial Y^2}+\frac{\partial^2}{\partial T^2}\right)\varphi-\kappa\varphi=-\kappa\varphi \tag{14}$$

where

$$\kappa=\frac{\tilde{\alpha}}{\alpha_f}. \tag{15}$$

4. GREEN'S FUNCTION

The weighting factors of the conventional objective analyses are comparable to the Green's function. The solution of eq (6) is written as follows:

$$\varphi(x,y,t)=\int_{-\infty}^{\infty}\int_{-\infty}^{\infty}\int_{-\infty}^{\infty}G(x,y,t;\xi,\eta,\tau)\kappa\tilde{\varphi}(\xi,\eta,\tau)d\xi d\eta d\tau \tag{16}$$

where G is Green's function,

$$G=\frac{1}{4\pi}\frac{e^{-\sqrt{\kappa}r}}{r} \tag{17}$$

and r is defined as

$$=r\left\{(x-\xi)^2+[(y-\eta)\cos\theta-(t-\tau)\sin\theta]^2+\frac{\alpha_f}{a+\alpha_f}[(y-\eta)\sin\theta+(t-\tau)\cos\theta]^2\right\}^{1/2}. \tag{18}$$

Derivation of the Green's function used in this paper and based on Schwartz' theory of the distribution is given in the appendix.

The Green's function is anisotropic if the translation velocity c_y does not vanish. Since the empirical weighting of the conventional objective analysis techniques is concerned with the x-y plane, it is interesting to investigate an (x,y) cross section of G where $t=\tau=$constant. The cross sectional pattern is denoted by $G_{x,y}$ and given from eq (17) as

$$G_{x,y}=\frac{1}{4\pi}\frac{e^{-\sqrt{\kappa}r_{x,y}}}{r_{x,y}} \tag{19}$$

where $r_{x,y}$ is written from eq (18) as

$$r_{x,y}=\{(x-\xi)^2+\left[\cos^2\theta+\frac{\alpha_f}{a+\alpha_f}\sin^2\theta\right](y-\eta)^2\}^{1/2}. \tag{20}$$

The eccentricity $\epsilon_{x,y}$ is given by

$$\epsilon_{x,y}=\left\{1-\left[\cos^2\theta+\frac{\alpha_f}{a+\alpha_f}\sin^2\theta\right]\right\}^{1/2}. \tag{21}$$

Since elongation is observed in the y-coordinate, the definition of the eccentricity is taken as eq (21). The eccentricity $\epsilon_{x,y}$ lies between 0 and 1. As $\epsilon_{x,y}$ approaches 1, the ellipse becomes more elongated along the y-coordinate.

Three numerical examples showing influences of c_y are given below:

(i) $c_y=0.1$,

$$r_{x,y}=\left\{(x-\xi)^2+\left(\frac{y-\eta}{1.005}\right)^2\right\}^{1/2}, \tag{22}$$

and the eccentricity $\epsilon_{x,y}$ is $\epsilon_{x,y}=0.07$;

(ii) $c_y=1.0$,

$$r_{x,y}=\left\{(x-\xi)^2+\left(\frac{y-\eta}{1.19}\right)^2\right\}^{1/2}, \tag{23}$$

and $\epsilon_{x,y}=0.541$; and

(iii) $c_y=10.0$,

$$r_{x,y}=\left\{(x-\xi)^2+\left(\frac{y-\eta}{3.17}\right)^2\right\}^{1/2}, \tag{24}$$

and $\epsilon_{x,y}=0.949$.

From these values of $r_{x,y}$, it is apparent that, as c_y decreases, the pattern of $G_{x,y}$ approaches a circle (axially symmetric with respect to the t-axis). As c_y increases, the $G_{x,y}$ pattern becomes elliptic, elongating equally in the upstream and downstream directions of the translation velocity. Also it is easily proven, although the discussion is omitted in this article, that as α_f decreases, the $G_{x,y}$ becomes more elliptic. A similar behavior for G is observed on the t-y cross section also.

5. ISOTROPIC WEIGHTING FACTORS AND GREEN'S FUNCTION

In most objective analysis methods, weighted smoothing is essential. The value of a meteorological parameter at a point (grid point) is determined from the weighted mean of the data at surrounding stations. The weighting factors are determined on empirical (or statistical) bases. The various methods differ essentially only in the choice of the weighting factors. Most weighting factor magnitudes decrease monotonically as the distance between the grid point and a station increases. Two types of weighting factors arise under this general system.

The weighting factor of the first type, W_1, is expressed by

$$W_1=\frac{1}{1+R_1^{2n}} \tag{25}$$

where n is an integer and R_1 is the normalized and nondimensional distance between the grid point and a station. The weights used by Bergthórsson and Döös (1955), Bushby and Huckle (1957), Barnes (1964), and Endlich and Mancuso (1968) are in this type. Linear combinations of W_1 obtained by choosing proper values of n or repeated application of a weighting factor s assists in increasing the accuracy of analysis. The weighting factor monotonically approaches zero as R_1 increases toward infinity.

The weighting factors for the second type, W_2, monotonically decrease toward zero as the nondimensionalized and normalized distance R_2 approaches 1, namely,

$$\begin{aligned} &W_2=\frac{1-R_2^2}{1+R_2^2} && R_2<1 \\ \text{and}\quad &W_2=0 && R_2\geq 1. \end{aligned} \tag{26}$$

This type includes the methods by Cressman (1959), Stephens (1967), and Inman (1970).

To compare these two types of weighing factors with the Green's function derived in the appendix, we choose one from each type. These factors were chosen to be in anisotropic forms so that they can be used again in the next section, which concerns anisotropic weighting factors. Endlich and Mancuso's and Cressman's weighting factors are chosen for the first and second types, respectively. The first one may be written as

$$W_1=\frac{1}{1+\left(\frac{r_1'}{c}\right)^2}=\frac{1}{1+R_1^2} \tag{27}$$

where c is a constant length dimension of 3 deg. lat. for the surface-map analysis and 6 deg. lat. for upper air analysis, and r_1' is the dimensional distance in deg. lat. between a grid point and a station. Endlich and Mancuso include a wind velocity term that gives more weight to the data in both the upstream and downstream direction as compared to the crosswind direction, but for simplicity the term is neglected in this section.

Cressman's weight, which was extended by Inman (1970) to include the anisotropic term, wind velocity, may be written as

$$\begin{aligned} &W_2=\frac{1-\left(\frac{r_2'}{R'}\right)^2}{1+\left(\frac{r_2'}{R'}\right)^2}=\frac{1-R_2^2}{1+R_2^2} && r_2'<R' \\ \text{and}\quad &W_2=0 && r_2'\geq R' \end{aligned} \tag{28}$$

where R' is the dimensional radius of influence and r_2' is the dimensional distance between a grid point and a station.

Using the empirical weighting factors, (27) and (28), the analyzed value $\varphi_{1,2}(x,y)$ using our notation is given by

$$\varphi_{1,2}(x,y)=\frac{\sum^N\tilde{\varphi}(\xi,\eta,\tau_0)\,W_{1,2}}{\sum^N W_{1,2}} \tag{29}$$

where $W_{1,2}$ represents W_1 or W_2, $\tilde{\varphi}(\xi,\eta,\tau_0)$ is the observed value at a specified time, $\tau_0=t_0$ (constant) at the point $Q(\xi,\eta,\tau_0)$, N is the total number of data stations, Σ is the sum taken over all stations, and $\varphi_{1,2}$ (x,y) is the analyzed value at $P(x,y,t_0)$ obtained by use of two different weighting factors as denoted by the subscripts 1 and 2.

Equation (29), which uses the empirical weighting factors, is similar to the one derived from the use of the Green's function eq (16). Since the following relationship is valid,

$$\begin{aligned} &\int_{-\infty}^{\infty}\int_{-\infty}^{\infty}\int_{-\infty}^{\infty}\kappa G(x,y,t;\xi,\eta,\tau)d\xi d\eta d\tau \\ &\qquad=\int_0^{2\pi}d\varphi\int_0^{\pi}\sin\theta d\theta\int_0^{\infty}\kappa\frac{e^{-\sqrt{\kappa}r}}{4\pi r}r^2dr=1, \end{aligned} \tag{30}$$

eq (16) can be rewritten

$$\varphi(x,y,t)=\frac{\int_{-\infty}^{\infty}\int_{-\infty}^{\infty}\int_{-\infty}^{\infty}\kappa G(x,y,t;\xi,\eta,\tau)\tilde{\varphi}(\xi,\eta,\tau)d\xi d\eta d\tau}{\int_{-\infty}^{\infty}\int_{-\infty}^{\infty}\int_{-\infty}^{\infty}\kappa G(x,y,t;\xi,\eta,\tau)d\xi d\eta d\tau}. \tag{31}$$

Comparing eq (31) with eq (29), $\kappa G(x,y,t;\xi,\eta,\tau)$ is

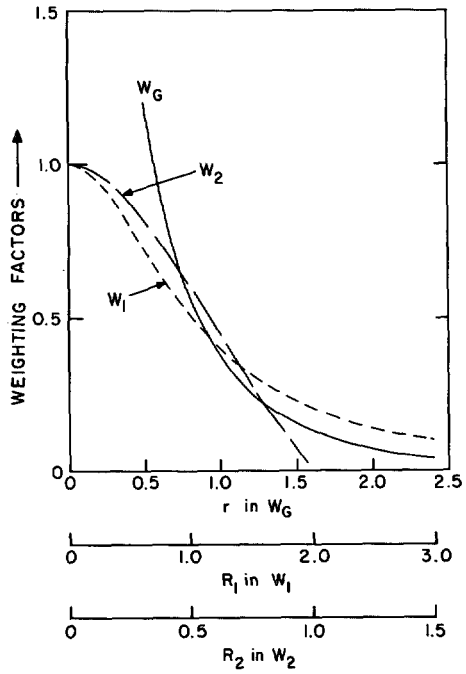

FIGURE 2.—Comparison of the empirical weighting factors W_1 and W_2 with the Green's function-oriented weighting factor W_G.

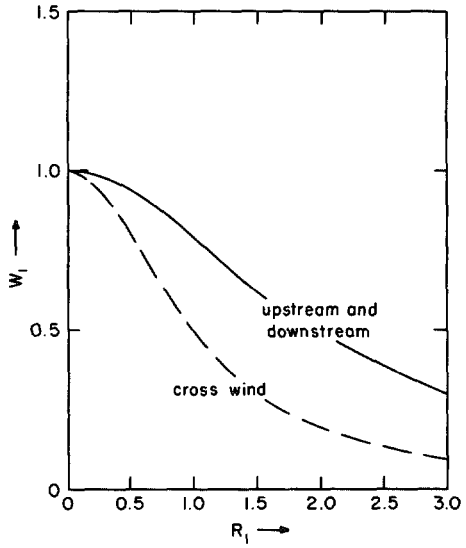

FIGURE 3.—Effect of $|\mathbf{R}_1 \times \mathbf{V}|$ on the anisotropy of W_1.

equivalent to empirical weighting factors W_1 and W_2. Let us use a notation W_G for the weighting factor determined by Green's function,

$$W_G = \kappa G(x,y,t;\xi,\eta,\tau). \tag{32}$$

Figure 2 shows a comparison among W_1, W_2, and W_G. The solid curve represents W_G where κ is assumed to be 1. The short dashed curve is W_1 and the long dashed curve shows W_2. The abscissae are r or $r^*[\equiv(x-\xi)^2+(y-\eta^2)]$, R_1, and R_2, respectively, for W_G, W_1, and W_2 where proper scaling factors have been used to bring all curves within close proximity to each other. Due to the unique nature of the three-dimensional Green's function, W_G increases toward infinity as r or r^* approaches zero, while the empirical weighting factors approach unity. The singularity of G or W_G at $r^*=0$ is an unfavorable feature for numerical calculations of $\varphi(x,y,t)$. In actual analysis, however, eq (5) will be used instead of eq (31) and no singularity appears.

6. ANISOTROPIC WEIGHTING FACTORS

Endlich and Mancuso (1968) gave greater weight to the data in the upstream and downstream directions than for the crosswind direction data. Their weighting factor, the isotropic version of which was discussed in section 5, may be written as

$$W_1 = \frac{1}{1+(|\mathbf{R}_1|+|\mathbf{R}_1 \times \mathbf{V}|)^2} \tag{33}$$

where $\mathbf{R}_1$ is the nondimensional position vector, $\mathbf{V}$ is the nondimensional and normalized wind vector (wind vector divided by a maximum wind speed in the area of interest). The magnitude of $|\mathbf{R}_1 \times \mathbf{V}|$ lies between 0 and $\mathbf{R}_1$. Figure 3 illustrates the effects of the anisotropic term $|\mathbf{R}_1 \times \mathbf{V}|$ on W_1. If the term is zero, W_1 becomes isotropic and the same as that in figure 2. The magnitude of the anisotropic W_1 is as much as two and one-half times that for the isotropic case. The eccentricity is high in this case.

Cressman's weighting factor, eq (28), is extended by Inman (1970) using the same idea as Endlich and Mancuso's in order to give more weight to both the upstream and downstream data. Inman's weighting factor may be expressed as

$$\begin{aligned} W_2 &= \frac{1-R_2^2}{1+R_2^2} \qquad R_2<1 \\ W_2 &= 0 \qquad\qquad R_2 \geq 1 \end{aligned} \tag{34}$$

R_2 is the nondimensionalized distance between a station and a grid point, as defined by

$$R_2 = \frac{d}{R^*}, \tag{35}$$

where d is the dimensional distance and R^* is the dimensional radius of influence. R^* includes a wind velocity term defined as

$$R^* = R(1+\beta \cos^2 \theta). \tag{36}$$

R is the radius of influence in the crosswind direction, θ is the angle between the position vector locating an observation from a grid point, and the wind velocity vector at the grid point, β, is a nondimensional ratio of the wind speed relative to a maximum wind speed as given by

$$\beta = \frac{bV}{V_m}; \tag{37}$$

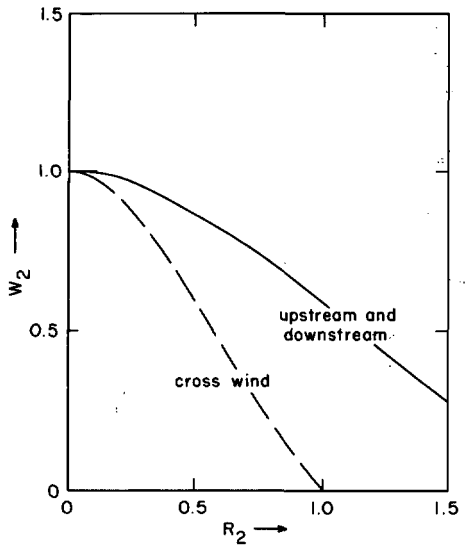

FIGURE 4.—Anisotropy of W_2.

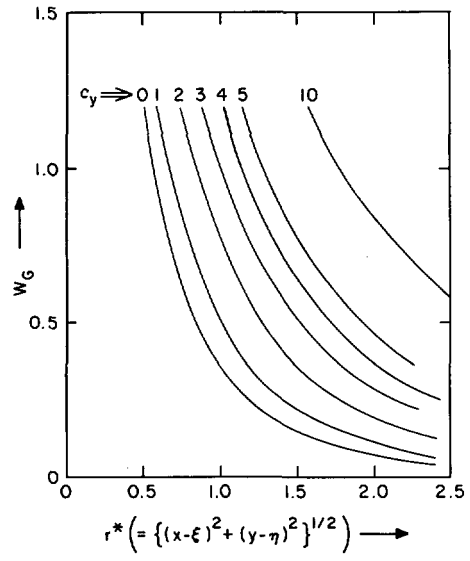

FIGURE 5.—Anisotropy of W_G as a function of the nondimensional wind speed.

b is a constant, usually unity. Figure 4 shows the weighting factor W_2 in the crosswind direction ($\beta=0$) and in the upstream and downstream directions ($\beta=1$). The eccentricity of W_2 is even higher than that of W_1.

Finally, the anisotropic nature of G or W_G can be compared with those of W_1 and W_2. The anisotropy of G and $G_{x,y}$ for this case, is given in eq (22), (23), and (24). The anisotropy of W_G should be the same as G. Figure 5 shows W_G in the upstream or downstream direction as functions of the nondimensional wind speed c_y. As seen from eq (20), the effective radius is increased in the upstream or downstream direction at the rate of $\{\cos^2\theta+[\alpha_f/(a+\alpha_f)]\sin^2\theta\}^{-1/2}$ times the isotropic radius. For example, the rate is 1.005 when $c_y=0.1$; 1.19 when $c_y=1.0$; and 3.17 when $c_y=10.0$ as shown in eq (22), (23), and (24), respectively. A choice of $L=100$ km and $\tau=3$ hr or $L=1000$ km and $\tau=30$ hr is reasonable for characteristic length and time scales. For both combinations, the characteristic scale of wind speed is 10 m/s. Hence, $c_y=1$ and 10 represents 10 m/s and 100 m/s, respectively. The rate of increase of the effective radius suggested from Green's function, i.e., 1.19 times for $c_y=10$ m/s and 3.17 for 100 m/s, seems to be in good agreement with the rate of 2.0 (regardless of the magnitude of c_y) used by Endlich and Mancuso (1968) and Inman (1970). It is also clear from the above analysis that isotropic weighting is generally sufficient when the wind speed is less than about 10 m/s.

7. PROPOSED DETERMINATION OF A TIME WEIGHTING FACTOR

Increasing importance has been placed on development of automated schemes for analyzing time series data at various observation stations. The empirical weighting factors, especially those proposed in the past and used in operational analyses, are designed for smoothing observations on a horizontal plane (x-y plane). It seems useful to investigate some guidelines for extending the presently existing weighting factors to include time series observavations. Green's function derived in this study is a weighting function not only of the horizontal coordinates x and y but also the time coordinate t, and seems to provide guidance for the desired extension.

(i) $G_{x,t}$; an x-t Cross Section of Green's Function

First, we investigate an x-t cross section of Green's function. From eq (17) and (18), G on an x-t cross section is written

$$G_{x,t}=\frac{1}{4\pi}\frac{e^{-\sqrt{\kappa}r_{x,t}}}{r_{x,t}} \tag{38}$$

where

$$r_{x,t}=\left\{(x-\xi)^2+\left[\sin^2\theta+\frac{\alpha_f}{a+\alpha_f}\cos^2\theta\right](t-\tau)^2\right\}^{1/2}. \tag{39}$$

This result represents the isolines of G as being elliptic and having the time coordinate t as the major axis and x as the minor axis since $\sin^2\theta+[\alpha_f/(a+\alpha_f)]\cos^2\theta$ is always less than 1, 0.5, 0.70, and 0.995, respectively, for $c_y=0$, 1, and 10 when $\alpha=\alpha_t=\alpha_s=\alpha_f=1$. The focal points are all on the time coordinate and located at ±1, ±0.65, and ±0.10, respectively, for $c_y=0$, 1, and 10. Figure 6 illustrates the above results.

It should be especially noted that the ellipticity or elongation along the t-axis in the case where $c_y=0$ results simply because the numerical values of α, α_t, α_s, and α_f are all chosen to be unity. In other words, the conditions $c_y=0$ and $\alpha=\alpha_t=\alpha_s=\alpha_f$ give

$$r_{x,t}=\left\{(x-\xi)^2+\left(\frac{y-\eta}{\sqrt{2}}\right)^2\right\}^{1/2}. \tag{40}$$

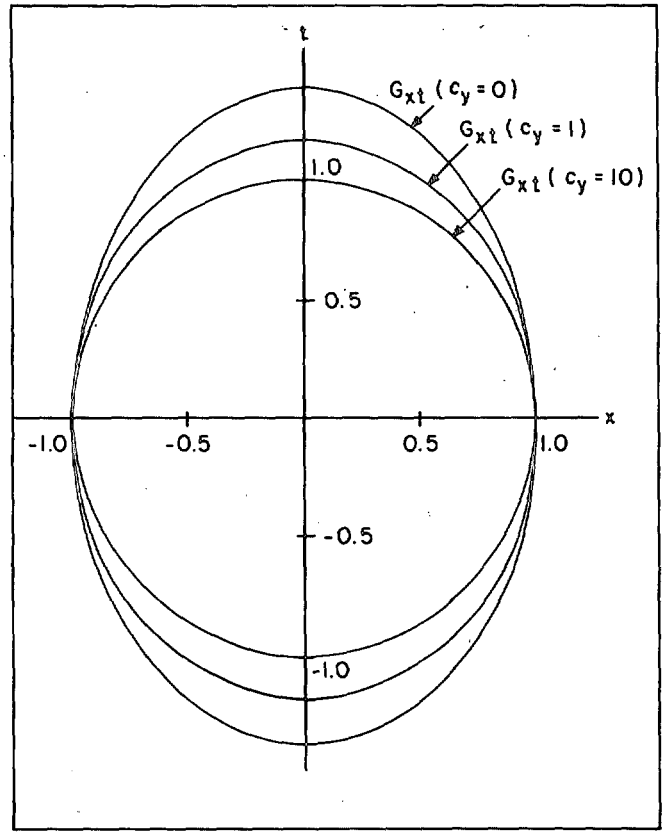

FIGURE 6.—Anisotropy of $G_{x,y}$ for various nondimensional wind speeds.

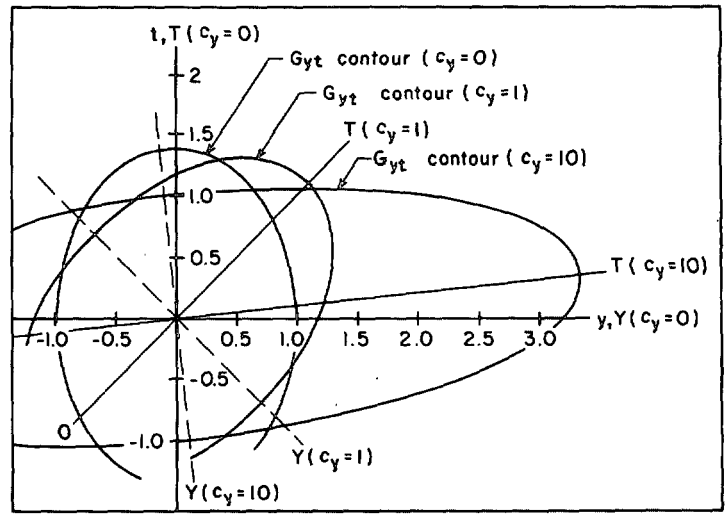

FIGURE 7.—Anisotropy of $G_{y,t}$ for various nondimensional wind speeds.

This choice of α's implies $\sqrt{2}$ times more smoothing in frequency (in time coordinate) than in wave number (in space coordinate when $c_y=0$). For equal smoothing in both the time and the space coordinates, proper and unequal choices of α's are necessary. For instance, the choice $\alpha_t=0$ and $\alpha_s=\alpha$ gives an isotropic pattern of G in the x-t or y-t cross sections when $c_y=0$.

(ii) $G_{y,t}$; a y-t cross section of Green's function

The pattern of G on a y-t cross section is expressed by taking $x=\xi=$const., as

$$G_{y,t}=\frac{1}{4\pi}\frac{e^{-\sqrt{\alpha}r_{y,t}}}{r_{y,t}} \tag{41}$$

where

$$r_{y,t}=\left\{[(y-\xi)\cos\theta-(t-\tau)\sin\theta]^2+\frac{\alpha_f}{a+\alpha_f}[(y-\xi)\sin\theta+(t-\tau)\cos\theta]^2\right\}^{1/2}. \tag{42}$$

This case is also similar to (i), since $G_{y,t}$ shows elliptic profiles on the y-t cross section. However, both major and minor axes rotate clockwise by the angle θ. After the rotation, the coordinates that coincide with the major and minor axes are denoted by X, Y, and T in the previous sections. The T coordinate (note that this is a characteristic line also) is enlarged by a factor of $(a+\alpha_f)/\alpha_f$ which is always larger than 1. These characteristics of $G_{y,t}$ for the three cases of $c_y=0$, 1, and 10 are shown in figure 7. The isolines of $G_{y,t}$ are all for $G_{y,t}=0.36$. This figure shows that as the wind speed increases, more weighting is necessary in the y-direction (in the upstream and downstream directions in space) and less weighting (the minimum is 1) is required in the time coordinate. Both figures 6 and 7 seem to encourage extension of the existing empirical weighting factors to include the time coordinate.

As discussed previously, the ellipticity of isolines of $G_{x,t}$ in figure 6 is merely due to the particular choice of α, α_t, and α_s. The effect of wind speed does not appear in $G_{x,t}$ in the cross section which is perpendicular to wind direction in the x-t plane. However, the effect of wind speed is apparent and significant as seen in figure 7 along the y-axis, which is taken as the wind direction in the y-t plane. Accordingly, it is suggested from this study that the possible weighting factors with respect to the time coordinate may be chosen in the same manner as the weighting factors in the crosswind direction.

APPENDIX

GREEN'S FUNCTION ON THE BASIS OF SCHWARTZ' THEORY OF DISTRIBUTION

The theory of distributions originally developed by Schwartz (1948, 1950, 1951) is also called the theory of ideal functions (Courant and Hilbert 1962). This theory provides a foundation for ideal functions such as Dirac's function and clarifies in its application the theoretical basis of Green's function. We apply the theory and associated mathematical techniques to derive Green's function for eq (14).

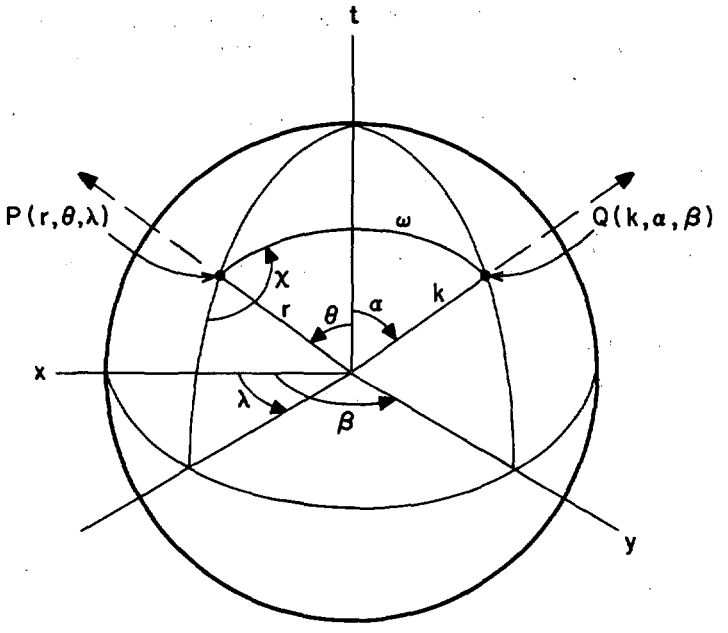

FIGURE 8.—Coordinate transformations of the (k_X,k_Y,k_T) and $(X-X',\ Y-Y',\ T-T')$ spaces to (k,α,β) and (r,θ,λ) spaces, respectively.

Equation (14) is rewritten

$$L[\varphi]\equiv\left(\frac{\partial^2}{\partial X^2}+\frac{\partial^2}{\partial Y^2}+\frac{\partial^2}{\partial T^2}-\kappa\right)\varphi=-\kappa\tilde{\varphi} \tag{43}$$

where L is the operator expressed by ( ) in eq (43). Let us first consider the elementary solution G_0 of the equation

$$L[G_0]=-\delta(X-X')\delta(Y-Y')\delta(T-T') \tag{44}$$

where the $(X-X')$, $(Y-Y')$, and $(T-T')$ are three components of the distance vector between two points $P(X,Y,T)$ and $Q(X',Y',T')$, δ is the Dirac's δ-function, namely $\delta(X-X')$ satisfies the following conditions

$$\begin{aligned}&\text{(i)}\ \delta(X-X')=0 \qquad X\neq X'\\ &\text{(ii)}\ \delta(X-X')=\infty \qquad X=X'\\ &\text{(iii)}\ \int_{-\infty}^{\infty}\delta(X-X')dX=1\end{aligned} \tag{45}$$

and similarly for $\delta(Y-Y')$ and $\delta(T-T')$. Schwartz called G_0 the "solution élémentaire" (elementary solution) which is a solution of eq (44) but it will be obtained without considering prespecified boundary conditions. The elementary solution is similar to the fundamental solution, but differs as the nonhomogeneous part of eq (43) is replaced by the δ-function.

The Fourier integral expression of the δ-function is

$$\delta(X-X')=\frac{1}{2\pi}\int_{-\infty}^{\infty}e^{ik_X(X-X')}dk,\quad -\infty<X,\ X'<\infty. \tag{46}$$

Similar expressions can be obtained for $\delta(Y-Y')$ and $\delta(T-T')$. If one uses eq (19), the right-hand side of eq (44), except for the sign, becomes

$$\begin{aligned}&\delta(X-X')\delta(Y-Y')\delta(T-T')\\ &=\frac{1}{(2\pi)^3}\int_{-\infty}^{\infty}\int_{-\infty}^{\infty}\int_{-\infty}^{\infty}e^{i\{k_X(X-X')+k_Y(Y-Y')+k_T(T-T')\}}dk_Xdk_Ydk_T.\end{aligned} \tag{47}$$

Let us assume a similar expression for G_0 where

$$\begin{aligned}G_0(X,Y,T;X',Y',T')=&\frac{1}{(2\pi)^3}\int_{-\infty}^{\infty}\int_{-\infty}^{\infty}\int_{-\infty}^{\infty}g(k_X,k_Y,k_T)\\ &\times e^{i\{k_X(X-X')+k_Y(Y-Y')+k_T(T-T')\}}dk_Xdk_Ydk_T.\end{aligned} \tag{48}$$

This Fourier integral expression is general and valid if the number of discontinuities of G_0 is finite.

Substitution of eq (47) and (48) into eq (44) leads to the relationships,

$$g(k_X,k_Y,k_T)=\frac{1}{k_X^2+k_Y^2+k_T^2+\kappa} \tag{49}$$

and

$$\begin{aligned}G_0(X,Y,T;X',Y',T')=&\frac{1}{(2\pi)^3}\int_{-\infty}^{\infty}\int_{-\infty}^{\infty}\int_{-\infty}^{\infty}\\ &\times\frac{e^{i\{k_X(X-X')+k_Y(Y-Y')+k_T(T-T')\}}}{(k_X^2+k_Y^2+k_T^2+\kappa)}dk_Xdk_Ydk_T.\end{aligned} \tag{50}$$

Additional coordinate transformations of eq (50) are made in the (k_X,k_Y,k_T) and $(X-X',Y-Y',T-T')$ spaces (fig. 8), namely to (k,α,β) and (r,θ,λ) where

$$\begin{aligned}k_X&=k\sin\alpha\cos\beta,\\ k_Y&=k\sin\alpha\sin\beta,\\ k_T&=k\cos\alpha,\end{aligned} \tag{51}$$

and

$$\begin{aligned}X-X'&=-r\sin\theta\cos\lambda,\\ Y-Y'&=-r\sin\theta\sin\lambda,\\ T-T'&=-r\cos\theta.\end{aligned} \tag{52}$$

The quantities ω and χ are defined as indicated in figure 8. Using the above newly defined independent variables, the following relationships are derived:

$$\begin{aligned}&k_X(X-X')+k_Y(Y-Y')+k_T(T-T')\\ &\quad=-kr\{\cos\theta\cos\alpha+\sin\theta\sin\alpha\cos(\lambda-\beta)\}=-kr\cos\omega\end{aligned} \tag{53}$$

and

$$\sin\alpha d\alpha d\beta=\sin\omega d\omega dx. \tag{54}$$

Using these new independent variables, G_0 becomes

$$\begin{aligned}G_0&=\frac{1}{(2\pi)^3}\int_{-\infty}^{\infty}\int_{-\infty}^{\infty}\int_{-\infty}^{\infty}\frac{e^{i\{k_X(X-X')+k_Y(Y-Y')+k_T(T-T')\}}}{k_X^2+k_Y^2+k_T^2+\kappa}dk_Xdk_Ydk_T\\ &=\frac{1}{(2\pi)^3}\int_0^{\infty}dk\int_{-\pi}^{\pi}dx\int_0^{\pi}\frac{e^{-ikr\cos\omega}}{k^2+\kappa}k^2\sin\omega d\omega\\ &=\frac{1}{(2\pi)^2}\int_0^{\infty}dk\int_0^{\pi}\frac{k^2e^{-ikr\cos\omega}}{k^2+\kappa}\sin\omega d\omega.\end{aligned} \tag{55}$$

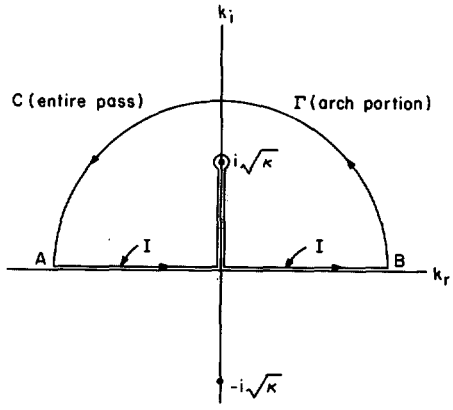

FIGURE 9.—The contour integral J of eq (62).

Since the following integration

$$\int_0^{\pi} e^{-ikr\cos\omega}\sin\omega d\omega = 2\frac{\sin kr}{kr} \tag{56}$$

is valid, G_0 is simplified as follows:

$$G_0 = \frac{2}{(2\pi)^2}\int_0^{\infty}\frac{k^2\sin kr}{(k^2+\kappa)kr}\,dk \tag{57}$$

and this is written, for convenience of the subsequent contour integral, as

$$G_0 = \frac{1}{(2\pi)^2}\int_{-\infty}^{\infty}\frac{k\sin kr}{(k^2+\kappa)r}\,dk. \tag{58}$$

Now consider the integral

$$I = \int_{-\infty}^{\infty}\frac{ke^{ikr}}{(k^2+\kappa)r}dk. \tag{59}$$

The relationship between G_0 and I is given as

$$G_0 = \frac{1}{(2\pi)^2}\mathrm{Im}\,(I) \tag{60}$$

where Im (I) is the imaginary part of I. In order to perform the integration expressed by eq (59), we assume k is a complex number defined by

$$k = k_r + ik_i \tag{61}$$

and we consider the following contour integral on the k-plane,

$$J = \oint_C \frac{ke^{ik_r r}e^{-k_i r}}{(k^2+\kappa)}\,dk. \tag{62}$$

Since $r \geq 0$ and the interval is finite in the upper half domain ($k_i > 0$), the integral pass C is taken as shown in figure 9. This pass is a sum of the integral on Γ (which is the upper half circle having the ends A and B), and the integral on the pass between A and B which makes it equal to eq (59). We exclude the singularity point $k = i\sqrt{\kappa}$ by taking pass C. The integral around the singularity gives the residue. Since the integral J should vanish along the entire pass C and the integral along Γ also vanishes as $r \to \infty$, we obtain

$$I = -\{-2\pi i\ \mathrm{Res}\ (i\sqrt{\kappa})\}. \tag{63}$$

Now the residue (Res) is

$$\mathrm{Res}\ (i\sqrt{\kappa}) = \lim_{k\to i\sqrt{\kappa}}(k-i\sqrt{\kappa})\frac{e^{ikr}}{(k+i\sqrt{\kappa})(k-i\sqrt{\kappa})r} = \frac{e^{-\sqrt{\kappa}r}}{2r}. \tag{64}$$

Accordingly,

$$I = i\pi\frac{e^{-\sqrt{\kappa}r}}{r} \tag{65}$$

and

$$G_0 = \frac{1}{(2\pi)^2}\mathrm{Im}(I) = \frac{1}{4\pi}\frac{e^{-\sqrt{\kappa}r}}{r} \tag{66}$$

where

$$r = \sqrt{(X-X')^2+(Y-Y')^2+(T-T')^2}. \tag{67}$$

The elementary solution of eq (44) is given by eq (66). The next step is to satisfy the boundary condition by linear addition of G_1 and G_2 to G_0

$$G = G_0 + C_1G_1 + C_2G_2 \tag{68}$$

where C_1 and C_2 are constant and G_1 and G_2 are solutions of the homogeneous part of eq (44)

$$L[G_l] = 0 \qquad l = 1, 2. \tag{69}$$

The boundary condition is chosen for the physical reason that the influence should vanish as the distance r approaches infinity, as follows:

$$G \to 0 \qquad r \to \infty. \tag{70}$$

Since G_0 satisfies this boundary condition, C_1 and C_2 are zero. Green's function of eq (43), G, which is now equal to G_0, is given by eq (66).

Finally, we transform the coordinates (X, Y, T) back to (x, y, t) through eq (7) and eq (13), and rewrite the Green's function in the following form,

$$G = \frac{1}{4\pi}\frac{e^{-\sqrt{\kappa}r}}{r} \tag{71}$$

where

$$r = \left\{(x-\xi)^2+[(y-\eta)\cos\theta-(t-\tau)\sin\theta]^2 + \frac{\alpha_f}{a+\alpha_f}[(y-\eta)\sin\theta+(t-\tau)\cos\theta]^2\right\}^{1/2} \tag{72}$$

and θ and a are given by eq (10) and eq (12).

Green's function, eq (71), satisfies the required condition

$$\lim_{r\to 0}\int_{\Gamma_r}\frac{\partial G}{\partial r}\,dS = -1 \tag{73}$$

where dS is an element of a surface, Γ_r, encircling the point $P(x, y, t)$ with an infinitesimal radius r. The proof of eq (73) is given as follows. From eq (71), the left-hand side of eq (73) becomes

$$\lim_{r\to 0}\int_{\Gamma_r}\frac{\partial G}{\partial r}\,dS=\lim_{r\to 0}\int_0^{2\pi}d\varphi\int_0^{\pi}\frac{1}{4\pi}\frac{\partial}{\partial r}\left(\frac{e^{-\sqrt{\kappa}r}}{r}\right)r^2\sin\theta\,d\theta$$

$$=\lim_{r\to 0}\left(-\sqrt{\kappa}\,re^{-\sqrt{\kappa}r}-e^{-\sqrt{\kappa}r}\right)=-1.$$

ACKNOWLEDGMENTS

This study was supported by the Environmental Science Services Administration (now the National Oceanic and Atmospheric Administration, NOAA) under Grants E22-19-69(G) and E22-43-70(G) and by the National Science Foundation under Grant NSF GA-238 which was awarded under the U.S.-Japan Science Cooperation program.

The author would like to express his sincere appreciation to the National Severe Storms Laboratory and the Meteorological Satellite Laboratory, both in NOAA, and the National Science Foundation, for their support and encouragement. Thanks are also due Dr. S. L. Barnes, National Severe Storms Laboratory, and Dr. R. L. Inman, University of Oklahoma, for their helpful discussions, and Mr. Robert C. Sheets, National Hurricane Research Laboratory and Dr. E. M. Wilkins, University of Oklahoma, for their critical reading of the manuscript. The author is grateful to Mrs. K. Amrein for her assistance in preparation of the manuscript.

REFERENCES

Barnes, Stanley L., "A Technique for Maximizing Details in Numerical Weather Map Analysis," *Journal of Applied Meteorology*, Vol. 3, No. 4, Aug. **1964**, pp. 396–409.

Bergthórsson, Páll, and Döös, Bo R., "Numerical Weather Map Analysis," *Tellus*, Vol. 7, No. 3, Stockholm, Sweden, Aug. **1955**, pp. 329–340.

Bushby, F. H., and Huckle, Vera M., "Objective Analysis in Numerical Forecasting," *Quarterly Journal of the Royal Meteorological Society*, Vol. 83, No. 356, London, England, Apr. **1957**, pp. 232–247.

Courant, Richard, and Hilbert, David, *Methods of Mathematical Physics*, Vol. II, Partial Differential Equations, Interscience Publishers, Inc., New York, N.Y., **1962**, 830 pp.

Cressman, George P., "An Operational Objective Analysis System," *Monthly Weather Review*, Vol. 87, No. 10, Oct. **1959**, pp. 367–374.

Endlich, R. M., and Mancuso, R. L., "Objective Analysis of Environmental Conditions Associated With Severe Thunderstorms and Tornadoes," *Monthly Weather Review*, Vol. 96, No. 6, June **1968**, pp. 342–350.

Inman, Rex L., "Operational Objective Analysis Schemes at the National Severe Storms Forecast Center," *Technical Circular* No. 10, National Severe Storms Laboratory, Environmental Science Services Administration, Norman, Okla., Feb. **1970**, 50 pp.

Sasaki, Yoshikazu, "Some Basic Formalisms in Numerical Variational Analysis," *Monthly Weather Review*, Vol. 98, No. 12, Dec. **1970***a*, pp. 875–883.

Sasaki, Yoshikazu, "Numerical Variational Analysis With Weak Constraint and Application to Surface Analysis of Severe Storm Gust," *Monthly Weather Review*, Vol. 98, No. 12, Dec. **1970***b*, pp. 899–910.

Schwartz, Laurent, "Généralisation de la Notion de Fonction et de Dérivation: Théorie des Distributions," *Annales de Télécommunications*, Vol. 3, No. 4, Centre National d' etude Télécommunications, Paris, France, **1948**, pp. 135–140.

Schwartz, Laurent, *Théorie des Distributions I*, Vol. I, Hermann, Paris, France, **1950**, 148 pp.

Schwartz, Laurent, *Théorie des Distributions II*, Vol. II, Hermann, Paris, France, **1951**, 161 pp.

Stephens, J. J., "Filtering Responses of Selected Distance-Dependent Weight Functions," *Monthly Weather Review*, Vol. 95, No. 1, Jan. **1967**, pp. 45–46.

[*Received June 10, 1970; revised October 15, 1970*]